Mesomorphic Behavior and Optical Properties of Liquid-Crystalline Polysiloxanes Bearing Different Chiral Groups

Fan-Bao Meng, Bao-Yan Zhang, Jiao Lian, Yan-Peng Wu, Xi-Zhi Li, Dan-Shu Yao

The Research Centre for Molecular Science and Engineering, Northeastern University, Shenyang 110004, People's Republic of China

Received 19 January 2007; accepted 18 March 2009
DOI 10.1002/app.30437
Published online 2 July 2009 in Wiley InterScience (www.interscience.wiley.com).

ABSTRACT: A series of side-chain liquid crystalline polysiloxanes bearing different chiral groups were synthesized with a cholesteric liquid crystalline monomer cholesteryl 2-(4-allyloxy-benzoxy)-succinate and a chiral monomer 2-isopropyl-5-methyl-cyclohexyl 4-allyloxy-benzoate. All the chiral polymers showed cholesteric mesophase with very wide mesophase temperature ranges. Along with phase morphology varied from solid state to isotropic state, the sample exhibited varied spectroscopic images, indicating different phase behaviors between mesophase and isotropic state. Optical properties of the polymers were characterized with circular polarization spectra and optical rotation analysis. The specific rotations of the chiral liquid crystalline polymers were all negative values and increased with increase of menthyl component in the polymer systems. As compared with corresponding monomers, the polymers showed significantly lower specific rotations, suggesting that the existence of polysiloxane main chains affect the molecule polarity. The selective light reflection maximum wavelength of the polymers at the same temperature shifted to short wavelength with decrease of cholesteryl component, indicating that the helical pitch becomes shorter due to induction of menthyl groups with high chiral properties. The temperature dependence of selective light reflection maximum wavelength was shifted to a longer wavelength region as the temperature decreased. © 2009 Wiley Periodicals, Inc. J Appl Polym Sci 114: 2195–2203, 2009

Key words: LCP; polysiloxanes; chiral phase behavior

INTRODUCTION

Chiral materials have been an extensively studied area in the field of materials science ever since the observation of their optical activity in the early 19th century. Most applications of chiral systems are based on their unique properties, which are directly related to the atomic chiral centers and helical conformations. As a type of special chiral materials, helical polymers have attracted attention due to their chiral structure and the resulting chiro-optical properties.[1] In synthetic chiral polymers, controlling the molecular helicity can be achieved by not only varying the molecular chirality but also via repeating units, hydrogen bonding, side chains, and block copolymers. In some cases, the molecular helicity can even be turned by environmental factors such as temperature, solvents, initiators, light, etc.[2]

When molecular chirality is introduced into liquid-crystalline (LC) polymers, chiral LC phases having helical morphology are induced, resulting in a series of potential applications in optics and electro-optics.[3–11] Chiral LC polymers may exhibit a marvelous variety of liquid crystalline phases, including the chiral smectic C* phase, the cholesteric phase, and the blue phases.[12–16] Recently, chiral side-chain LC polymers (CSLCPs) composed of chiral mesogens have attracted both industrial and scientific interests, because their additional properties such as piezoelectricity, Ferro electricity, and pyroelectricity result from the symmetry breaking brought by molecular chirality.[17–22] Furthermore, the basic research on optical properties and its application of CSLCPs has grown substantially. The detailed relationship between the structure and optical properties of CSLCPs remains unclear so far. Therefore, it is of interest to synthesize novel CSLCPs and study the relationship between the structure and optical properties of CSLCPs.

To achieve a better understanding of the influence of molecular structure on the helical twist sense and optical properties, we are interested in chiral LCPs prepared with chiral LC monomers and other polymerizable groups. In the present study, a series of

Correspondence to: B.-Y. Zhang (byzcong@163.com).
Contract grant sponsor: NSFC; contract grant number: 50873018.
Contract grant sponsors: Program for New Century Excellent Talents in University, China Postdoctoral Science Foundation, and Educational Science and Technology Program of Liaoning Province (Education Department and Science and Technology Department of Liaoning Province).

polysiloxane-based CSLCPs were graft polymerized by a cholesteric LC monomer and a chiral non-LC monomer bearing different chiral groups.

EXPERIMENTAL

Materials and measurements

2-Hydroxy-succinic acid, *p*-hydroxybenzoic acid, cholesterol, menthol, bromopropene, hexachloroplatinic acid hydrate, and poly(methylhydrogeno)siloxane (PMHS) (M_n = 600–800) were obtained from Jilin Chemical Industry Company (Jilin City, China) and used without any further purification. Pyridine, thionyl chloride, chlorethyl alcohol, toluene, ethanol, chloroform, tetrahydrofuran (THF), and methanol were purchased from Shenyang Chemical (Shenyang City, China) Pyridine was purified by distillation over KOH and NaH before using.

FTIR spectra of the synthesized polymers and monomers in solid state were obtained by the KBr method performed on Perkin Elmer Instruments Spectrum One Spectrometer (Perkin Elmer, Foster City, CA). ^{1}H-NMR (300 MHz) spectrum was obtained with a Varian Gemini 300 NMR Spectrometer (Varian Associates, Palo Alto, CA) with Fourier transform with dimethyl sulfoxide-d_6 (DMSO-d_6) or $CDCl_3$ as a solvent and tetramethylsilane (TMS) as an internal standard. The element analyses (EA) were carried out by using an Elementar Vario EL III (Elementar, Hanau, Germany). Thermal transition properties were characterized by a NETZSCH instruments DSC 204 (Netzsch, Wittelsbacherstr, Germany) at a heating rate of 10°C min^{-1} under nitrogen atmosphere. Phase transition temperatures were collected during the second heating and the first cooling scans. Visual observation of liquid crystalline transitions and optical textures under cross-polarized light was made with a Leica DMRX (Leica, Wetzlar, Germany) POM equipped with a Linkam THMSE-600 (Linkam, Surrey, England) hot stage. X-ray diffraction (XRD) of the samples was performed using Cu Kα (λ = 1.542 Å) radiation monochromatized with a Rigaku DMAX-3A X-ray diffractometer (Akishima, Tokyo, Japan). Circular polarization spectra were measured by Perkin Elmer Instruments Lambda 950. Measurement of optical rotation (α) was carried out with a Perkin Elmer Instrument Model 341 Polarimeter using the D line of a sodium vapor lamp. FTIR imaging analysis was acquired using a Perkin Elmer Instrument Spectrum spotlight FTIR imaging system.

Synthesis of LC monomer cholesteryl 2-(4-allyloxy-benzoxy)-succinate (M1)

Scheme 1 shows the synthesis route of chiral monomers including **M1**. 4-Allyloxy-benzoxy acid was synthesized according to a reported procedure.[23] 4-Allyloxy-benzoic acid (20.0 g, 0.11 mol), 35 mL thionyl chloride, and 1.0 mL of pyridine were added into a round flask equipped with an absorption instrument of hydrogen chloride. The mixture was stirred at room temperature for 3 h, then heated to 60°C and kept for 4 h in a water bath to ensure that the reaction finished. The excess thionyl chloride was distilled under reduced pressure. Then, 50 mL of cold chloroform was added to the residue at 25°C to obtain chloroform solution of 4-allyloxy-benzoyl chloride (**1**). 2-Hydroxy-succinic acid (13.4 g, 0.10 mol) and 8 mL pyridine were dissolved in 70 mL of dry chloroform. It was added dropwise with chloroform solution of **1** at 25°C. The reaction mixture was stirred at room temperature for 2 h, then heated to 60°C and kept for 6 h in a water bath to ensure that the reaction was finished. After cooling to room temperature, the mixture was poured into 200 mL cold alcohol. The precipitates were isolated by filtration and dried in a vacuum oven. Recrystallization in alcohol results in white crystals of 2-(4-allyloxy-benzoxy)-succinic acid (**2**).

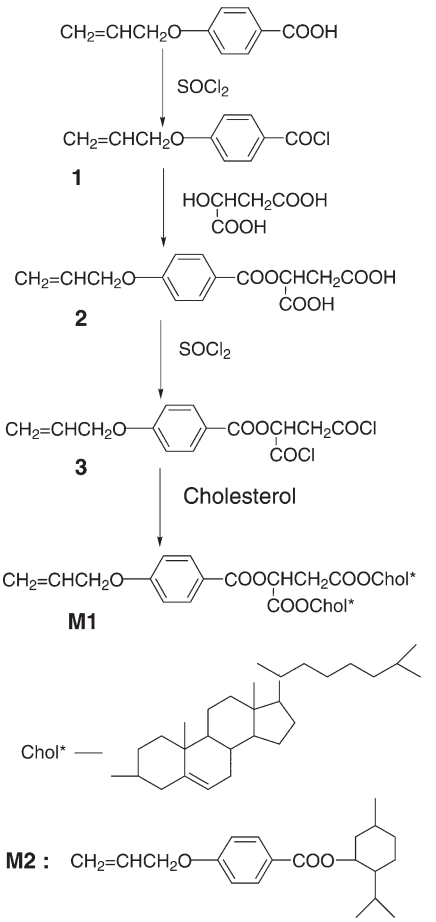

Scheme 1 Synthesis routes of the liquid crystalline and chiral monomers.

Yield: 75%. m.p.: 173°C. IR (KBr, cm^{-1}): 3050, 2920, 2848 (—CH_2—, CH_2= and =CH), 2682, 2583

(—OH stretching in —COOH), 1721 (C=O in ester linkage), 1690 (C=O in —COOH), 1601, 1505 (Ar), 1273 (C—O—C). ^{1}H-NMR (DMSO-d_6, δ, ppm): 2.85–2.92 [d, 2H, —CH_2COOH—]; 4.55–4.65 (m, 2H, =CHCH_2—); 5.01–5.13 [m, 1H, —OCH(CH$_2$—) COO—]; 5.20–5.28 (m, 2H, CH_2=CH—); 5.83–5.90 (m, 1H, CH$_2$=CH—); 6.90–7.85 (m, 4H, Ar—H); 10.01–10.12 (s, 2H, —COOH).

The compound **2** (32.4 g, 0.11 mol), 35 mL thionyl chloride, and 1.5 mL of pyridine were added into a round flask equipped with an absorption instrument of hydrogen chloride. The mixture was stirred at room temperature for 4 h, then heated to 60°C and kept for 5 h to ensure that the reaction finished. The excess thionyl chloride was distilled under reduced pressure. Then, 60 mL of cold chloroform was added to the residue at 25°C to obtain chloroform solution of 2-(4-allyloxy-benzoxy)-succinoyl chloride (**3**). Cholesterol (77.4 g, 0.20 mol) and 16 mL pyridine were dissolved in 280 mL dry chloroform. It was added dropwise with chloroform solution of **3** at room temperature. The reaction mixture was stirred at room temperature for 1 h, then heated to 60°C and kept for 8 h in a water bath to ensure that the reaction was finished. Then, 250 mL of chloroform was distilled out. After cooling to room temperature, the mixture was poured into cold alcohol. The precipitates were isolated by filtration and dried in a vacuum oven. Recrystallization in THF results in white crystals of liquid crystalline monomer cholesteryl 2-(4-allyloxy-benzoxy)-succinate (**M1**).

Yield: 65%. $[\alpha]_D^{20} = -30.8°$, $c = 1$, chloroform, m.p.: 113.6°C. IR (KBr, cm^{-1}): 2925, 2855 (—CH$_2$—, CH$_2$= and =CH), 1727, 1715, (C=O), 1605, 1506 (Ar), 1273 (C—O—C). Elem. Anal. Calcd. for $C_{70}H_{106}O_7$: C, 79.35%; H, 10.08%. Found: C, 79.48%; H, 10.13%. ^{1}H-NMR (CDCl$_3$, δ, ppm): 0.99–2.16 (m, 92H, CH_3—, —CH_2—, and —CH— in cholesteryl groups); 4.01–4.59 (m, 4H, =CHCH_2O— and cholesteryl —CH— in ester linkage); 5.15–5.24 (m, 4H, CH_2=CH— and =CH— in cholesteryl groups); 5.73–5.91 (m, 1H, CH$_2$=CH—); 6.95–7.94 (m, 4H, Ar—H).

Synthesis of chiral monomer 2-isopropyl-5-methyl-cyclohexyl 4-allyloxy-benzoate (M2)

Menthol (15.6 g, 0.10 mol) and 10.0 mL dry pyridine were dissolved in 100 mL dry chloroform to form a solution. The chloroform solution of 4-allyloxy-benzoyl chloride (0.11 mol) was added dropwise to the solution and reacted at 60°C for 28 h; some solvent was then distilled out. The mixture was cooled and poured into 200 mL of cold alcohol. The precipitated crude product was filtered, recrystallized with alcohol, and dried overnight under vacuum to obtain a white powder of chiral monomer 2-isopropyl-5-methyl-cyclohexyl 4-allyloxy-benzoate (**M2**).

TABLE I
Polymerization and Specific Rotation of the Polymers

Sample	Feed			$[\alpha]_D^{20}$[a]
	PMHS (mmol)	M1 (mmol)	M2 (mmol)	
1P	0.250	1.750	0.000	−3.951
2P	0.250	1.575	0.175	−4.278
3P	0.250	1.400	0.350	−4.545
4P	0.250	1.225	0.525	−4.813
5P	0.250	1.050	0.700	−6.452
6P	0.250	0.875	0.875	−7.132
7P	0.250	0.700	1.050	−7.175

[a] Specific rotation of polymers, 0.1 g in 10 mL CHCl$_3$.

Yield: 73%. $[\alpha]_D^{20} = -48.6°$, $c = 1$, chloroform, m.p.: 18°C. IR (KBr, cm^{-1}): 2925, 2835 (—CH$_2$—, CH$_2$= and =CH), 1727 (C=O), 1605, 1503 (Ar), 1298 (C—O—C). Elem. Anal. Calcd. for $C_{20}H_{28}O_3$: C, 75.91%; H, 8.92%. Found: C, 76.04%; H, 8.83%. ^{1}H-NMR (CDCl$_3$, δ, ppm): 0.99–1.10 (m, 9H, —CH_3); 1.28–1.99 (m, 9H, —CH_2—, and —CH— in menthyl group); 3.96–4.59 [m, 3H, =CHCH_2O— and —OCH(CH$_2$—)(CH—)]; 5.11–5.22 (m, 2H, CH_2=CH—); 5.75–5.92 (m, 1H, CH$_2$=CH—); 6.92–7.95 (m, 4H, Ar—H).

Synthesis of the polymers

For synthesis of polymers **1P–7P**, the same method was adopted. The polymerization experiments and specific rotations are summarized in Table I. The synthesis of polymer **3P** is given as an example. Chiral LC monomer **M1** (1.40 mmol) was dissolved in 50 mL of dry, fresh distilled toluene. To the stirred solution, chiral monomer **M2** (0.35 mmol), PMHS (0.25 mmol), and 2 mL of H_2PtCl_6/THF (0.50 g hexachloroplatinic acid hydrate dissolved in 100 mL THF) were added and heated under nitrogen and anhydrous conditions at 65°C for 28 h. The mixture was then cooled and poured into methanol. After filtration, the product was dried at 80°C for 4 h under vacuum to obtain polymer in the yield of 92%.

RESULTS AND DISCUSSION

Syntheses

The synthetic routes for the target monomers are shown in Scheme 1. The structures of **M1** and **M2** were characterized by IR and ^{1}H-NMR spectra, which was in good agreement with the prediction. The spectra of **M1** and **M2** suggest that the purity is high, and this was confirmed by elementary analysis.

Polymers **1P–7P** were prepared by a one-step hydrosilylation reaction between Si—H groups of PMHS and olefinic C=C of **M1** and **M2** in toluene,

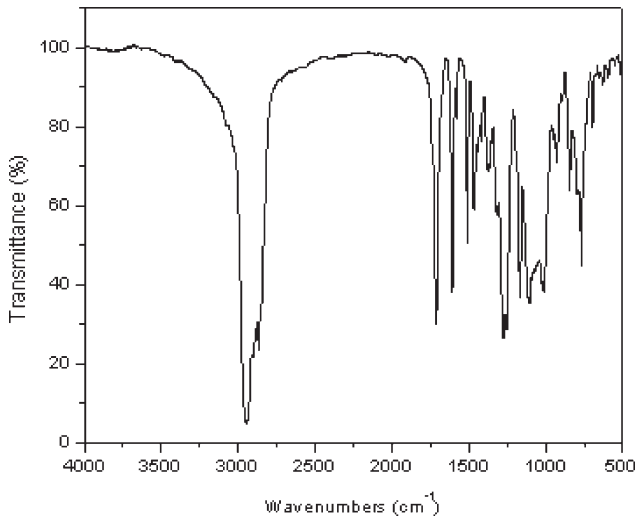

Figure 1 FTIR spectra of representative polymer **4P**.

with hexachloroplatinate (IV) as a catalyst. The obtained polymers were soluble in toluene, xylene, THF, chloroform, and so forth. Their structures were characterized by IR spectra. Polymer **4P** contains the representative features for all of the polymers, which are shown in Figure 1. The characteristic absorption bands are as follows: 2995–2847 cm^{-1} (C—H stretching), 1726–1715 cm^{-1} (C=O stretching in ester modes), 1610–1598, 1513–1499 cm^{-1} (aromatic stretching), 1199–1079 cm^{-1} (Si—O—Si stretching). The disappearance of the PMHS Si—H stretching at 2160 cm^{-1} and the olefinic C=C stretching band at 1635 cm^{-1} indicate successful incorporation of monomers into the polysiloxane chains. In addition, the ester C=O absorption bands on monomer **M1** and **M2** and the characteristic Si—O—Si broad stretching bands on PMHS still existed in the polymers.

FTIR imaging analysis

A powerful step forward in the field of vibrational spectroscopy was made by the introduction of Fourier transform infrared (FTIR) imaging. FTIR imaging offers a possibility of simultaneously measuring spectra from many different locations in the sample. These FTIR spectra provide information about the concentration of a specific compound and its chemical structure and morphology. FTIR spectroscopy also provides sample average measurements of the composition of multicomponent samples. As traditionally used, FTIR spectroscopy provides sample average measurements of the composition of multicomponent samples. Besides, FTIR microscopy has been used to map the spatial distribution of multiphase systems.[24–27] Therefore, it is possible to simultaneously measure and differentiate between the spatial distribution of composites in a polymer system or even of different morphologies of chemically identical substances, for example, amorphous and crystalline domains in polymers. Side-chain LC polymers have ordered molecular orientation of mesogens among the amorphous polymer systems; thus it is interesting to study the mesomorphic phase behaviors by use of FTIR imaging technology.

In this work, we applied the FTIR imaging technique to a spatial analysis of the morphology in the phase states. The samples were monitored from room temperature to temperature of anisotropic–isotropic transition at the heating rate 1.0°C min^{-1}. The infrared spectroscopic images of the sample **4P** exhibiting different phase behaviors at different temperatures were taken from the Spectrum Spotlight FTIR imaging system. In consideration of the mesogens in LC states bearing benzene ring structure, the aromatic stretching (1610–1598 cm^{-1}) modes from the sample were identified. Figure 2 shows the morphologies on heating circles of **4P**. From the comparison of spectra at different temperatures, the differences in total absorbance intensities in the aromatic stretching modes were used as probes for FTIR imaging contrasts. Along with phase morphology varied from solid state to isotropic state, the sample exhibited varied spectroscopic images, indicating different phase behaviors between mesophase and isotropic state. When it was heated from 30 to 125°C, the infrared spectroscopic images did not change greatly, showing that the glass transition does not change the arrangement of benzene rings. When the sample was heated to 130°C, the aromatic stretching began to dissociate, indicating ordered molecular orientation of mesogens bearing benzene rings among the amorphous polymer systems, and the phase morphology varied from solid state to mesomorphic state. With increased temperature under isotropic temperature, the aromatic stretching weakened slightly, as shown in Figure 2(d,e). When it was heated above the isotropic temperature, the aromatic stretching dissociated and weakened greatly, as displayed in Figure 2(f), suggesting disorder arrangement of benzene rings.

Thermal analysis

The phase-transition temperatures and corresponding enthalpy changes of LC monomer **M1** and the LCPs **1P–7P**, obtained on the second heating and the first cooling scan, are summarized in Table II. All phase transitions were reversible and did not change on repeated heating and cooling cycles. DSC thermograms of **M1** and representative curves of the polymers are presented in Figures 3 and 4, respectively.

DSC curves of **M1** showed a melting transition and a cholesteric–isotropic phase transition at 113.6 and 258.1°C on heating and displayed anisotropic–

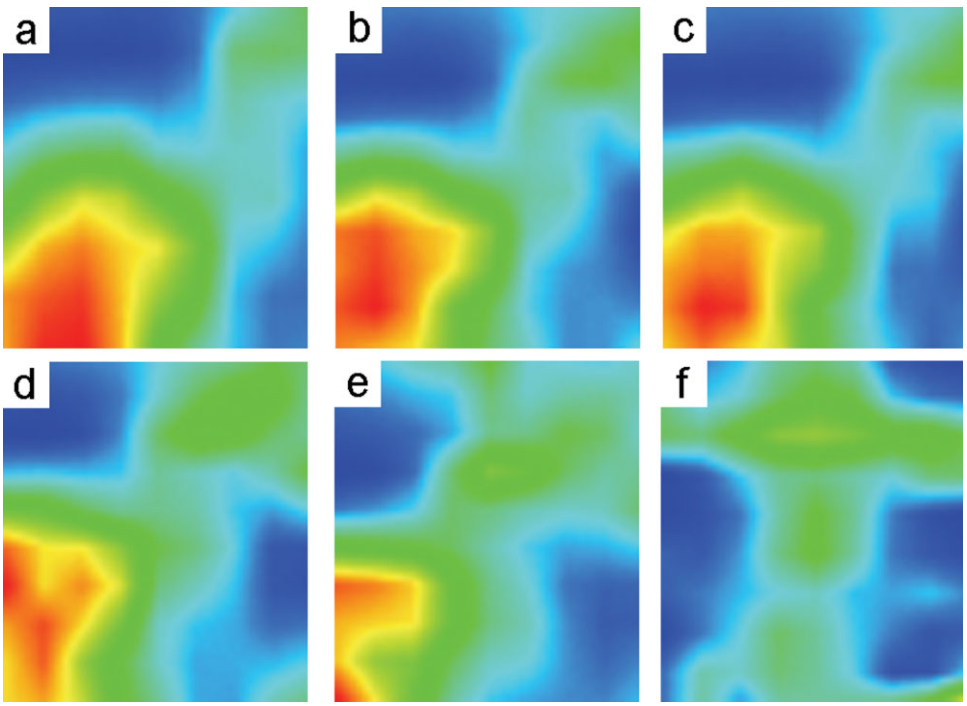

Figure 2 Infrared spectroscopic images of heating cycles for **4P** on heating rate 1.0°C min^{-1} at (a) 30°C; (b) 51°C; (c) 80°C; (d) 130°C; (e) 180°C; and (f) 250°C. [Color figure can be viewed in the online issue, which is available at www.interscience.wiley.com.]

cholesteric phase transition and crystallization process at 231.2°C and 92.4°C on cooling, respectively.

DSC thermograms of all the polymers showed a glass transition, a melt transition, and an LC phase to isotropic transition, respectively. The glass transition temperature (T_g) and the melting temperature (T_m) of all polymers did not change greatly with increase of **M2** in the polymer systems, whereas the isotropic temperature (T_i) decreased slightly on heating circles. Therefore, temperature range of mesophase decreased slightly from **1P** to **7P**. Side-chain LC polymers are most commonly composed of flexible and rigid moieties, thus the polymer backbone, the rigidity of mesogenic units, and the length of the flexible spacer would influence mesophase behaviors of the polymers. Because of the same polymer backbone and the similar length of the flexible spacer in **M1** and **M2**, all the polymers displayed similar T_g. However, mesogens decreased with increase of **M2** in the polymer systems, leading to decrease of T_i.

Texture analysis

The optical textures of the monomer **M1** and the polymers were studied by means of POM with hot stage, shown in Figure 5. POM results showed that

TABLE II
Some Thermal Properties of LC Monomer M1 and the Series of Polymers

	DSC heating					DSC cooling		
Sample	T_g (°C)	T_m (°C)	ΔH_m (J g^{-1})	T_i (°C)	ΔH_i (J g^{-1})	ΔT^a (°C)	$T_{i\text{-}Ch}{}^b$ (°C)	$T_{Ch\text{-}K}{}^c$ (°C)
M1	–	113.6	35.432	258.1	2.351	144.5	231.2	92.4
1P	30.5	124.8	3.452	245.0	3.516	120.2	244.2[d]	72.3
2P	28.9	124.1	3.551	244.6	2.868	120.5	240.2	73.5
3P	26.1	124.6	3.213	243.1	0.598	118.5	239.8	72.1
4P	33.8	125.3	3.784	240.8	1.235	115.5	236.2	80.6
5P	37.6	125.0	4.058	236.9	2.356	111.9	228.8	81.3
6P	36.7	125.2	3.965	231.6	1.974	106.4	226.4	82.8
7P	35.4	124.8	4.021	224.9	1.437	100.1	219.2	81.5

[a] Mesophase temperature ranges on heating.
[b] Phase transition from isotropic state to cholesteric mesophase.
[c] Phase transition from mesophase to solid.
[d] Observed from POM analysis.

M1 exhibited an enantiotropic cholesteric phase on heating and cooling cycles. When **M1** was heated to 248°C, the typical cholesteric oily streak texture appeared. When the melt was cooled to 238°C, it displayed focal conic texture of a short pitch mesophase separating from the isotropic melt, as shown in Figure 5(b).

All the chiral polymers showed tiny deformed focal conic textures and did not exhibit the characteristic oily streak texture of cholesteric mesophase, the reason for which is due to the higher viscoelasticity of the polymer systems. The representative optical textures of **1P** and **6P** are shown in Figure 5(c,d). Although the monomer **M2** did not show LC mesophase and it contained different chiral groups from **M1**, the chiral polymers still displayed cholesteric LC state.

XRD analysis

The cholesteric mesophase of the polymers was also characterized by XRD analysis. In general, a sharp and strong peak at low angle ($1° < 2\theta < 4°$) in small-angle X-ray scattering (SAXS) curves together with a strong broad peak associated with lateral packing at $2\theta \approx 20°$ in wide-angle X-ray diffraction (WAXD) curves can be observed for a smectic polymer structure. For nematic and cholesteric structure of polymer systems, no strong peak appeared in the SAXS curves. However, a broad peak at $2\theta \approx 20°$ and $2\theta \approx 17°$ was observed in the WAXD curves of nematic and cholesteric polymers, respectively.[28,29] Therefore, it is a very important characteristic for judging cholesteric structure that broad diffraction angles appear at lesser angles than those of nematic structures in WAXD. It suggests that the average distance between two neighbor LC molecules within the layers of the mesophase become broad due to the helix structure of cholesteric LC polymers. Figure 6 shows representative XRD curves of quenched samples of **1P**, **4P**, and **7P**. For all the polymers, no strong small angle reflection was observed, indicating that they did not show smectic mesophase. A broad peak appeared around $2\theta \approx 17°$, not at $2\theta \approx 20°$, for **1P–7P**, suggesting chiral helix structure between two neighbor LC molecules within the layers of the mesophase. Therefore, the cholesteric mesophase structure of **1P–7P** was confirmed by XRD results.

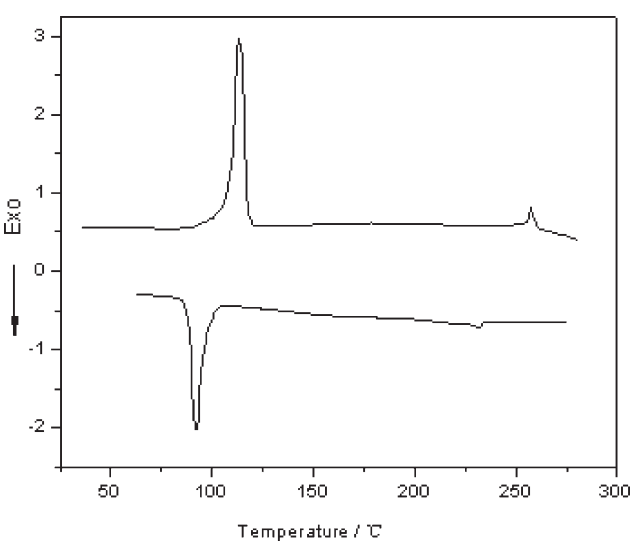

Figure 3 DSC thermograms of monomer **M1** on the second heating and the first cooling.

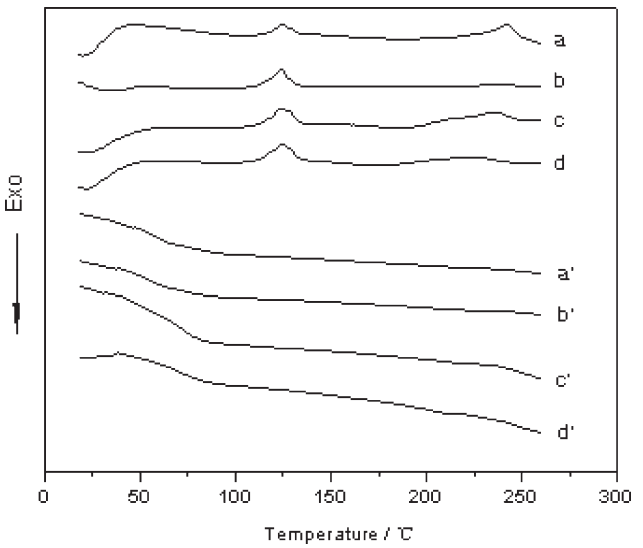

Figure 4 DSC thermograms of representative polymers on the second heating (a, **1P**; b, **3P**; c, **5P**; d, **7P**) and the first cooling (a′, **1P**; b′, **3P**; c′, **5P**; d′, **7P**).

Optical rotation analysis

The optical properties of chiral LCPs result from chiral molecules in the liquid crystalline state that induce a twist in the direction of adjacent molecules, thereby forming a super molecular helical structure. Therefore, it is interesting to study the variation of optical rotation (α) due to the introduction of different chiral groups in the side-chain LC polymers.

For the different chiral monomers, as can be seen in Scheme 1, cleavage of O—H bond of cholesterol and menthol occurred during the introduction of the cholesteryl and menthyl groups into **M1** and **M2**, respectively. Accordingly, the configuration of the cholesteryl and menthyl groups must be retained for all synthesized chiral compounds. As compared with cholesterol ($[\alpha] = -31.5°$) and menthol ($[\alpha] = -50.2°$), monomers **M1** and **M2** bearing phenyl segments showed significantly higher specific rotations. The results suggest that the existence of high-resonance phenyl segments might affect the molecule

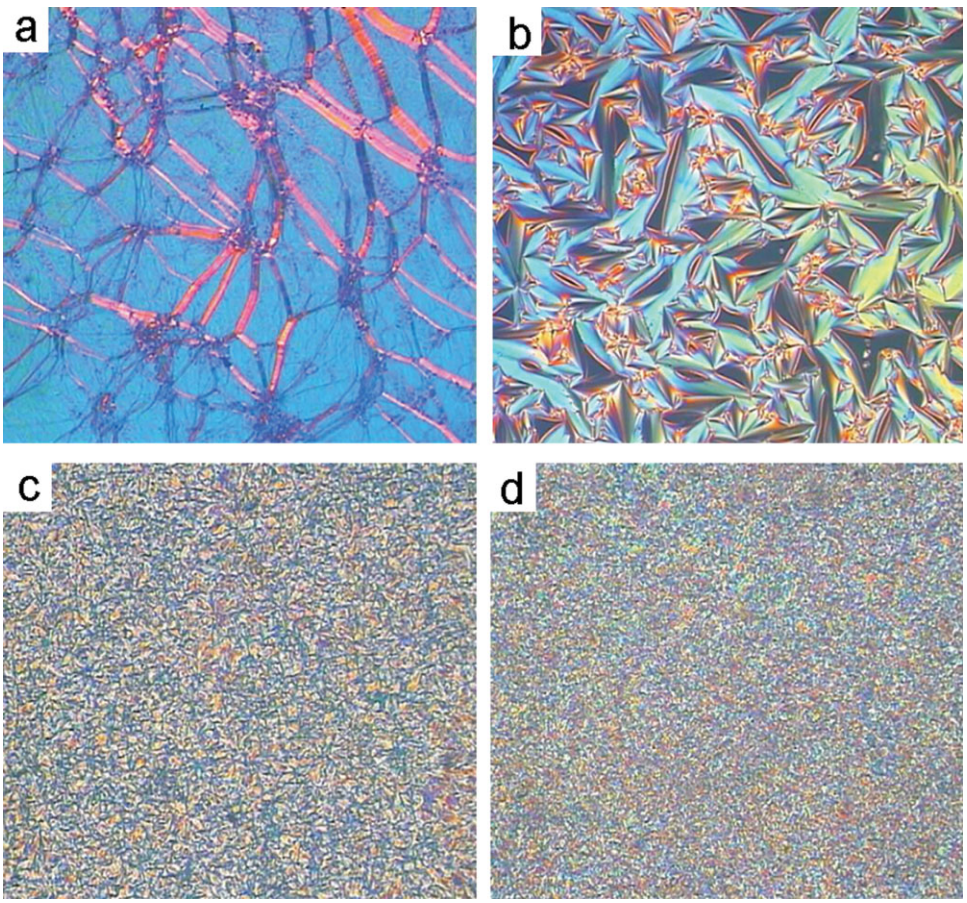

Figure 5 Optical texture of the monomer and polymers (×200): (a) oily streak texture of **M1** at heating to 248°C; (b) focal conic texture of **M1** at cooling to 238°C; (c) deformed focal conic texture of **1P** at heating to 158°C; and (d) deformed focal conic texture of **6P** at cooling to 163°C. [Color figure can be viewed in the online issue, which is available at www.interscience.wiley.com.]

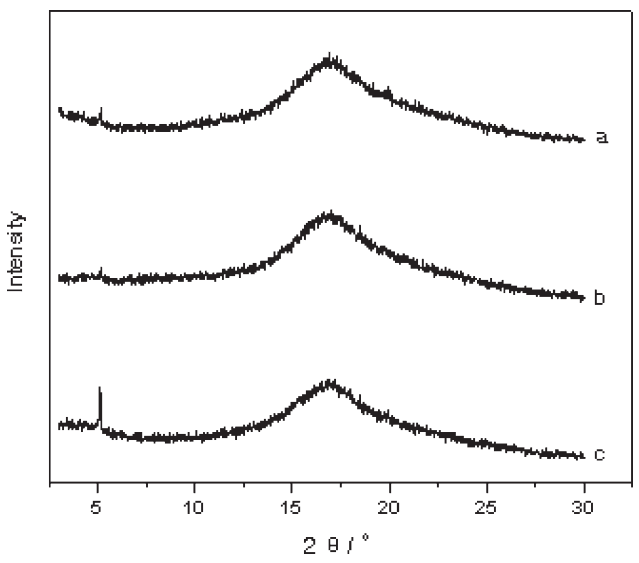

Figure 6 Representative XRD curves of polymers: (a) **1P**; (b) **4P**; and (c) **7P**.

polarity, leading to the decrease of the specific rotations.

Although the specific rotations of the chiral liquid crystalline polymers are all negative values, cleavage of the double bond and the binding of two monomers to the polysiloxane main chains appeared to significantly affect the chirality of the compounds, as shown in Table I. As compared with monomers **M1** ($[\alpha] = -30.8°$) and **M2** ($[\alpha] = -48.6°$), the polymers showed significantly lower specific rotations. The results suggest that the existence of polysiloxane main chains affect the molecule polarity, leading to the decrease of the specific rotations. As shown in Table I, the specific rotation of polymers from **1P** to **7P** revealed similar tendency, i.e., the specific rotation absolute values increasing with increase of the **M2** component in the polymer systems. The higher specific rotations absolute values of the **M2** component bearing menthyl groups in the pendant group of polymers might change chiral properties on the

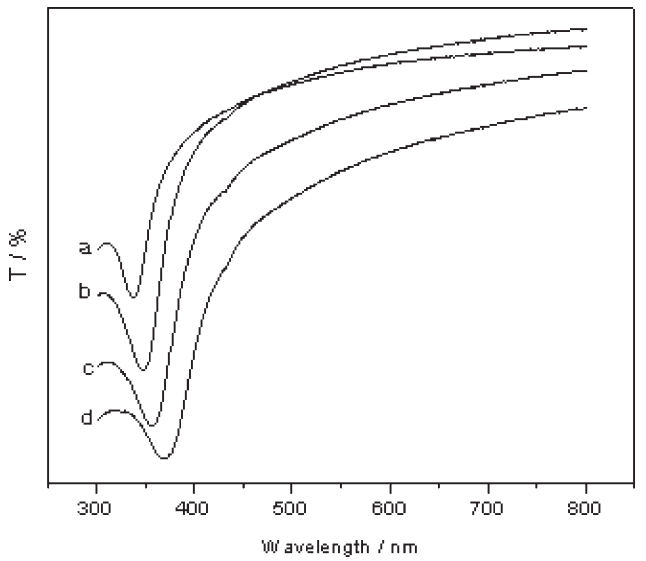

Figure 7 Circular polarization spectra of representative polymers at the same temperature (on heating to 165.0°C): (a) **7P**; (b) **5P**; (c) **3P**; and (d) **1P**.

polymers, leading to the increase of the specific rotation.

Circular polarization spectra analysis

Cholesteric mesophases exhibit interesting optical properties such as the selective reflection of circular polarized light and an angular dependence of the reflected wavelength. If the reflected wavelength is in the visible range of the spectrum, the cholesteric phase appears colored. The wavelength, λ_{max}, of reflected light from a cholesteric sample, is given by

$$\lambda = nP \sin \varphi \quad (1)$$

where n is the average refractive index of the liquid crystalline phase, P is the pitch height of the helicoidal arrangement, and φ is the incident angle of beam. The helical pitch is an important parameter in connection with optical properties of the cholesteric phase. Although the microscopic origins of the helical pitch are still a subject of study, it is known that the helical pitch and optical properties of side-chain cholesteric LC polymers mainly depend on the polymer backbone, the rigidity of mesogenic units, the length of the flexible spacer, and the outer condition (such as temperature, force field, electric field, and magnetic field).

For the polymers, although the typical oil streak texture of cholesteric phase did not form, the cholesteric phase was attested by the analysis of phase diagrams studying the polarization optical structures and XRD analysis. The transmission spectra of thin films (Figs. 7 and 8) show well-pronounced peaks of selective light reflection, and this trend unequivocally suggests the formation of cholesteric phase.

Let us consider in more detail the optical characteristics of the cholesteric phase of the polymers containing different chiral groups at the same temperature. In this case, as the liquid crystalline monomer **M1** component is decreased, selective light reflection maximum λ_{max} is shifted to a shorter wavelength region, as shown in Figure 7. According to eq. (1), as compared with the specific rotation absolute values increasing with increase of **M2** component in the polymer systems, the helical pitch becomes shorter due to induction of menthyl groups with high chiral properties, leading to blue shift of λ_{max}.

For the λ_{max} of cholesteric polymers at different temperature, as the temperature is decreased, λ_{max} is shifted to a longer wavelength region. Figure 8 presents the temperature dependence of λ_{max} for copolymer **4P** on cooling. For **4P** polymer matrices, with decreasing the temperature from isotropic to mesomorphic state, a dramatic untwisting of cholesteric helix takes place; as a result, selective light reflection maximum λ_{max} markedly increases as the temperature is decreased. This tendency may be explained by the formation of cholesteric order in the vicinity of the isotropic–cholesteric transition. Upon any further decrease in temperature, selective light reflection peak is fully degenerated, and this fact unequivocally attests to the development of the cholesteric solid transition.

CONCLUSIONS

A series of side-chain LC polysiloxanes bearing different chiral groups were synthesized by a cholesteric liquid crystalline monomer cholesteryl 2-(4-

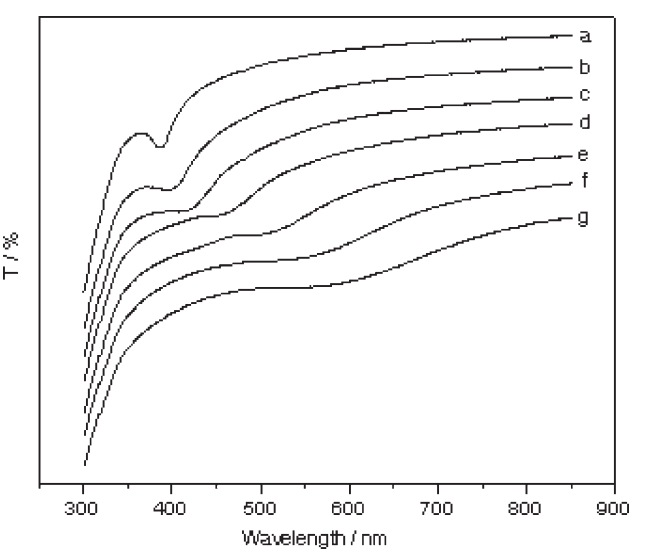

Figure 8 Circular polarization spectra of polymer **4P** on cooling cycles: (a) 180°C; (b) 140°C; (c) 120°C; (d) 100°C; (e) 80°C; (f) 60°C; and (g) 50°C.

allyloxy-benzoxy)-succinate and a chiral monomer 2-isopropyl-5-methyl-cyclohexyl 4-allyloxy-benzoate. The chemical structures and LC properties of the monomers and polymers were characterized by various experimental techniques including FTIR, ^{1}H-NMR, EA, DSC, POM, and XRD. All the chiral polymers showed cholesteric mesophase with very wide mesophase temperature ranges. Along with phase morphology varied from solid state to isotropic state, the sample exhibited varied spectroscopic images, indicating different phase behaviors between mesophase and isotropic states. Optical properties of the polymers were characterized with circular polarization spectra, optical rotation analysis, and FTIR imaging analysis.

The specific rotations of the chiral liquid crystalline polymers are all negative values. As compared with corresponding monomers, the polymers showed significantly lower specific rotations, suggesting that the existence of polysiloxane main chains affect the molecule polarity. The specific rotation absolute values of polymers increased with increase of menthyl component in the polymer systems.

The selective light reflection maximum λ_{max} of the polymers with different chiral groups at the same temperature shifted to short wavelength as the liquid crystalline monomer bearing cholesteryl component was decreased, indicating that the helical pitch becomes shorter due to induction of menthyl groups with high chiral properties. On the other hand, the temperature dependence of λ_{max} for polymers was shifted to a longer wavelength region as the temperature is decreased.

References

1. Mruk, R.; Zentel, R. Macromolecules 2002, 35, 185.
2. Weng, X.; Li, C. Y.; Jin, S.; Zhang, D.; Zhang, J. Z.; Bai, F.; Harris, F. W.; Cheng, S. Z. D. Macromolecules 2002, 35, 9678.
3. Walba, D. M.; Yang, H.; Shoemaker, R. K.; Keller, P.; Shao, R.; Coleman, D. A.; Jones, C. D.; Nakata, M.; Clark, N. A. Chem Mater 2006, 18, 4576.
4. Yamane, H.; Kikuchi, H.; Kajiyama, T. Polymer 1999, 40, 4777.
5. Lia, C. Y.; Gea, J. J.; Baia, F.; Zhanga, J. Z.; Calhouna, B. H.; Chienb, L. C.; Harrisa, F. W.; Lotzc, B.; Chenga, S. Z. D. Polymer 2000, 41, 8953.
6. Sikorski, P.; Cooper, S. J.; Atkins, E. D. T.; Jaycox, G. D.; Vogl, O. J Polym Sci Part A: Polym Chem 1998, 36, 1855.
7. Hwang, J. C.; Shu, M. C.; Lin, C. P. Macromol Chem Phys 1999, 200, 2250.
8. Li, C. Y.; Cheng, S. Z. D.; Ge, J. J.; Bai, F.; Zhang, J. Z.; Mann, I. K.; Chien, L.; Harris, F. W.; Lotz, B. J Am Chem Soc 2000, 122, 72.
9. Barmatov, E. B.; Barmatova, M. V.; Moon, B. S.; Park, J. G. Macromolecules 2004, 37, 5490.
10. Shibaev, V.; Bobrovsky, A.; Boiko, N. Prog Polym Sci 2003, 28, 729.
11. Amabilino, D. B.; Ramos, E.; Serrano, J.; Sierra, T.; Veciana, J. J Am Chem Soc 1998, 120, 9126.
12. Sun, S. J.; Schwarz, G.; Kricheldorf, H. R.; Chang, T. C. J Polym Sci Part A: Polym Chem 1999, 37, 1125.
13. Meng, F. B.; Zhang, B. Y.; Xiao, W. Q.; Hu, T. X. J Appl Polym Sci 2005, 96, 625.
14. Kricheldorf, H. R.; Krawinkel, T. Macromol Chem Phys 1998, 199, 783.
15. Kricheldorf, H. R.; Sun, S. J.; Chen, C. P.; Chang, T. C. J Polym Sci Part A: Polym Chem 1997, 35, 1611.
16. Schwarz, G.; Kricheldorf, H. R. J Polym Sci Part A: Polym Chem 1996, 34, 603.
17. Hsiue, G. H.; Chen, J. H. Macromolecules 1995, 28, 4366.
18. Hsu, L. L.; Chang, T. C.; Tsai, W. L.; Lee, C. D. J Polym Sci Part A: Polym Chem 1997, 35, 2843.
19. Hsiue, G. H.; Lee, R. H.; Jeng, R. J.; Chang, C. S. J Polym Sci Part B: Polym Phys 1996, 34, 555.
20. Hiraoka, K.; Stein, P.; Finkelmann, H. Macromol Chem Phys 2004, 205, 48.
21. Shilov, S.; Gebhard, E.; Skupin, H.; Zentel, R.; Kremer, F. Macromolecules 1999, 32, 1570.
22. Brodowsky, H. M.; Boehnke, U. C.; Kremer, F. Langmuir 1999, 15, 274.
23. Meng, F. B.; Zhang, B. Y.; Liu, L. M.; Zang, B. L. Polymer 2003, 44, 3935.
24. Kimura, K.; Kawai, Y.; Oosaki, S.; Yajima, S.; Yoshioka, Y.; Sakurai, Y. Anal Chem 2002, 74, 5544.
25. Bhargava, R.; Levin, I. W. Macromolecules 2003, 36, 92.
26. Oh, S. J.; Koenig, J. L. Anal Chem 1998, 70, 1768.
27. Challa, S. R.; Wang, S. Q.; Koenig, J. L. J Appl Spectrosc 1995, 49, 267.
28. Meng, F. B.; Zhang, B. Y.; Li, Q. Y. Polym J 2005, 37, 277.
29. Hu, J. S.; Zhang, B. Y.; Zhou, A. J.; Dong, Y. L.; Zhao, Z. X. J Polym Sci Part A: Polym Chem 2005, 43, 3315.